

VIII. PHYSICAL ACOUSTICS*

Prof. K. U. Ingard
 Dr. L. W. Dean III
 Dr. G. C. Maling, Jr.
 Dr. H. L. Willke, Jr.

B. L. Chrisman
 P. A. Fleury V
 K. W. Gentle
 G. M. Irwin
 A. A. Maduemezia

W. M. Manheimer
 J. H. Turner
 S. D. Weiner
 J. M. Witting

A. SOUND EMISSION FROM AN AMPLITUDE-MODULATED RADIOFREQUENCY DISCHARGE

The generation of sound waves by means of a modulated high-frequency discharge described in the last report¹ has been further investigated by measurements of the sound pressure generated as a function of the gas pressure. The modulated discharge is located at one end of a tube, and the sound is received at the other end. To prevent standing waves in the tube, the tube is terminated by absorptive material which prevents

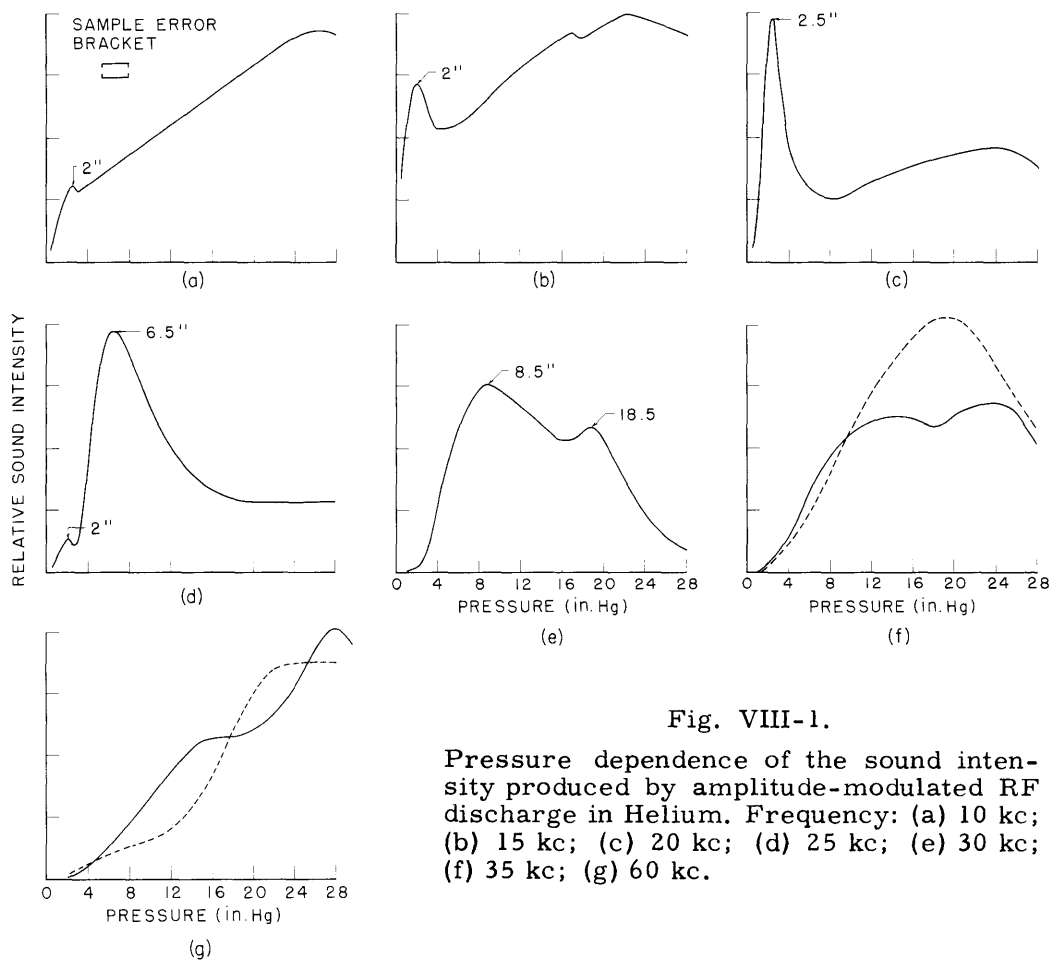


Fig. VIII-1.

Pressure dependence of the sound intensity produced by amplitude-modulated RF discharge in Helium. Frequency: (a) 10 kc; (b) 15 kc; (c) 20 kc; (d) 25 kc; (e) 30 kc; (f) 35 kc; (g) 60 kc.

*This work was supported in part by the U. S. Navy (Office of Naval Research) under Contract Nonr-1841(42).

(VIII. PHYSICAL ACOUSTICS)

sound reflection. A typical sequence of curves illustrating the pressure dependence on the acoustic intensity is given in Fig. VIII-1. These curves refer to generation into helium. It is interesting to note that a "resonance" occurs at a certain pressure, and the pressure at this resonance increases as the frequency increases. Similar results have been obtained for argon. This effect is not yet understood and further work is in progress.

B. L. Chrisman, G. M. Irwin, U. Ingard

References

1. B. L. Chrisman and G. M. Irwin, Investigation of ultrasonic coupling and relaxation effects at a corona-neutral gas interface, Quarterly Progress Report No. 73, Research Laboratory of Electronics, M.I.T., April 15, 1964, pp. 23-24.

B. FLOW STABILITY AND THE ENERGY IDENTITY

Difficulty with a class of perturbed flows of irregular time dependence, whose instability would seem to indicate creation of energy, has led to an investigation of the energy sources for unstable flows. It will be seen that, in an exact analysis, the total kinetic energy of perturbation tends to zero with time for perturbations not affecting the strength of the energy sources for the basic flow.

The energy identity for the Navier-Stokes equations is obtained formally as follows:

$$\begin{aligned} 0 &= \iiint_V d^3y v_i (\partial_t v_i - \nu \Delta v_i + v_j \partial_j v_i + \partial_i P) \\ &= \iiint_V d^3y \left[\partial_t \frac{v^2}{2} - \nu v_i \Delta v_i + v_j \partial_j \left(\frac{v^2}{2} + P \right) \right] \\ &= \iiint_V d^3y \left[\partial_t \frac{v^2}{2} + \nu (\partial_j v_i)^2 \right] + \iint_{\dot{V}} dS \left[-\nu v_i \partial_n v_i + v_n \left(P + \frac{v^2}{2} \right) \right]. \end{aligned} \quad (1)$$

Clearly, if $\nu \neq 0$, and if the boundary conditions on P and the v_i are so prescribed that the surface integrals in (1) vanish, then the v_i will tend to zero for large t . In particular, if v^2 is integrable, we have

$$\frac{\partial}{\partial t} \iiint_V \frac{v^2}{2} d^3y = -\nu \iiint_V (\partial_j v_i)^2 d^3y < 0,$$

so that $\iiint_V v^2 d^3y$ must continue to decrease in time as long as one of the

v_i is nonzero somewhere.

When applied to the stability problem for parallel flows, the energy identity demonstrates for us the nonexistence of spatially localized instabilities: plausibly enough, the perturbation must encompass an energy source for the basic flow.

If we suppose the basic parallel flow to be directed along the x_3 coordinate, we may write for the perturbed flow $v_i = u_i + W(x_1, x_2) \delta_{i3}$, $P = p + x_3 P_0$, with $-\nu \Delta W \delta_{i3} + \partial_i x_3 P_0 = 0$.

In order to avoid difficulties associated with an infinite total energy

$$\iint dx_1 dx_2 \int_{-\infty}^{\infty} dx_3 W^2$$

for the basic flow, we consider the term-by-term limit of the difference between the energy identities associated with the perturbed and unperturbed flows as we extend the domain of integration to the whole space. Supposing that the u_i are integrable and vanish at rigid boundaries and, for simplicity, that W is bounded, and suppressing in advance terms that vanish in the limit, we get

$$\begin{aligned} & \iiint_V d^3y \partial_t \left[\frac{v^2}{2} + \nu (\partial_j v_i)^2 - \nu (\partial_j W_i)^2 \right] + \iint_{\dot{V}} dS [-\nu W \partial_n u_3 + \delta_{n3} W p + \dots] \\ &= \iiint_V d^3y \left[\partial_t \frac{v^2}{2} + \nu (\partial_j u_i)^2 - 2\nu (\Delta W) u_3 \right] + \iint_{\dot{V}} dS [-\nu W \partial_n u_3 + \delta_{n3} W p + \dots] \\ & \rightarrow \iiint_{E^3} d^3y \left[\partial_t \frac{v^2}{2} + \nu (\partial_j u_i)^2 \right] + \iint_{\text{Boundaries}} dS [-\nu W \partial_n u_3] \\ & + \lim_{x_3 \rightarrow \infty} \int dx_1 \int dx_2 W [p(x_3) - p(-x_3)]. \end{aligned} \quad (2)$$

If there are no sliding boundaries, then $W|_{\text{Boundary}} = 0$, so that (2) gives us what we want: If $p(x_3) - p(-x_3) = o(1)$, then all surface contributions vanish, so that, with $\nu \neq 0$, $\iiint d^3y \frac{\partial}{\partial t} \frac{v^2}{2}$ is strictly negative as long as any of the u_i are nonzero. Under these conditions, v^2 cannot remain everywhere positive unless the u_i tend to zero almost everywhere in time. If sliding boundaries are admitted, these considerations hold only if $\partial_n u_3$ vanishes at such boundaries. In general, perturbations must couple to the energy sources for the basic flow if they are not to decay in time; that is, the surface terms must not vanish.

In the special case $\nu = 0$, the basic flow maintains itself without energy sources,

(VIII. PHYSICAL ACOUSTICS)

so $P_o = 0$, and it is no longer possible to extract energy from sliding boundaries. On the other hand, since no sources of dissipation exist, we have

$$\iiint \frac{\partial}{\partial t} \frac{v^2}{2} d^3y = 0,$$

even when the remaining surface term vanishes, so that the perturbed flow maintains itself in the mean.

H. L. Willke, Jr.

C. ACOUSTIC POWER RADIATED BY A MONOPOLE SOUND SOURCE IN A DUCT

The acoustic power (W) radiated by a sound source located near boundaries may be quite different from the power output in free space (W_o).^{1, 2} Ingard and Lamb¹ and Waterhouse² have dealt with sources near rigid surfaces. Solutions for W/W_o when the surface is partially reflecting have been presented by Grine,³ Maling,⁴⁻⁶ and Waterhouse⁷ for various boundary conditions. For a constant-strength (that is, constant mass flow) monopole the expression⁶ for W/W_o is

$$\frac{W}{W_o} = 1 + \frac{1}{kA} \text{Im}(p_r), \tag{1}$$

where $\text{Im}(p_r)$ is the imaginary part of the reflected pressure at the source. The source pressure is $p_s = (A/r) \exp(ikr)$, and k is the wave number, ω/c . The solutions for W/W_o that have been worked out thus far deal with sources between parallel walls, in a corner, and over an infinite plane.

One interesting extension of this work is a calculation of W/W_o for a point-monopole source in a duct. If the source is located at position (x_o, y_o, z_o) in a duct that has dimensions a and b in the x - y plane, and is infinite in the z -direction, the sound field can be shown to be

$$p(x, y, z) = 2\pi i \omega Q_o \sum_{k_x, k_y} \left\{ \frac{A_x^2 A_y^2}{(k^2 - k_x^2 - k_y^2)^{1/2}} \right\} \cdot \{ \cos(k_x x - \psi_x) \cos(k_x x_o - \psi_x) \cos(k_y y - \psi_y) \cos(k_y y_o - \psi_y) \} \exp(ik_z(z - z_o) - i\omega t), \tag{2}$$

where p is the sound pressure at the field point, Q_o is the strength of the source, ω is the frequency, k_x and k_y are solutions to $\tan(k_n L/2) = -ik\beta_n/k_n$ for the even modes, and $\cot(k_n L/2) = ik\beta_n/k_n$ for the odd modes. Here, n represents x or y , and L represents a or b . A_x and A_y are normalization constants, and $k_z = (k^2 - k_x^2 - k_y^2)^{1/2}$. Also,

$$\psi_n = -\tan^{-1} (ik\beta_n/k_n).$$

For hard walls in a duct ($\beta_n = 0$), and the power output of the source can be found by integration of the acoustic intensity in the propagating modes. For example, the ratio W/W_0 is $2\pi/k^2 ab$ for the plane-wave mode, and can be found easily for the higher modes. Thus, W/W_0 can be found as a function of k for a constant-strength source.

If the source is of the constant-pressure type, it is necessary to evaluate Eq. 2 near the source, and remove the asymptotic e^{ikr}/r dependence in order to find both the real and imaginary parts of the reflected pressure at the source. Both are needed because the mass flow produced by the source must adjust itself to keep the total pressure at the surface of the source constant.

If the duct walls are hard, or if a plane-wave reflection coefficient can be used to describe the effect of the boundary, an image description can be used to find the reflected pressure at the source. It can be shown that the ratio W/W_0 for a constant-pressure source of radius a is

$$\frac{W}{W_0} = \frac{1 + \frac{1}{k} \text{Im} (p_r)}{1 + 2a \text{Re} (p_r) + a^2 |p_r|^2}. \tag{3}$$

Note that p is assumed to be of the form e^{ikr}/r , and therefore has dimensions 1/length.

Image solutions have been found for a source in the center of a square duct with rigid

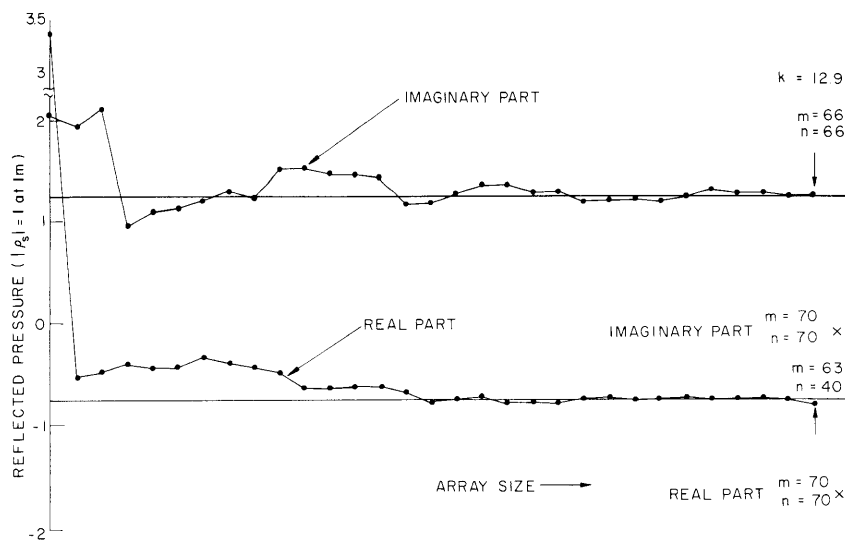


Fig. VIII-2. Real and imaginary parts of the reflected pressure at the source for $k = 12.9$. The abscissa is the array size, the points being those that satisfy the criteria that have been discussed.

(VIII. PHYSICAL ACOUSTICS)

walls (side length = L) by programming an IBM 7094 computer to sum up the images. The program was written so that the pressure field from groups of images (at least four images to a group) were printed out when the total image strength was less than one. This procedure insured that the convergence would be reasonably rapid. The cumulative total was printed out for these groups. A typical calculation is shown in Fig. VIII-2. The calculations are cut off when the array of images reaches 70×70 , and it can be seen that a 66×66 array (for the imaginary part of the pressure) and a 63×40 array (for the real part of the pressure) are much more consistent with earlier groups that meet the criterion discussed above than the 70×70 array calculation which does not. Thus, it is important to choose carefully the order in which the terms are taken to insure convergence of the partial sums of the series.

The ratio W/W_0 can be found for a constant-strength source either by use of the Green's function method described above, or by the summation of images. The latter method was used in the calculation of the curves shown in Fig. VIII-3. This plot emphasizes the difference between the power output of the constant-strength source in free space and the power output in a duct. An alternative method of treating the data is to plot the power output relative to its value at $k = 0$. This has been done, and the results are shown in Fig. VIII-4. It can be seen that coupling to the higher order modes is considerably stronger than the coupling to the plane-wave mode ($k < 6.28$ for the plane wave mode, the first cross mode is not excited).

For a constant-pressure source the image technique is most convenient, and,

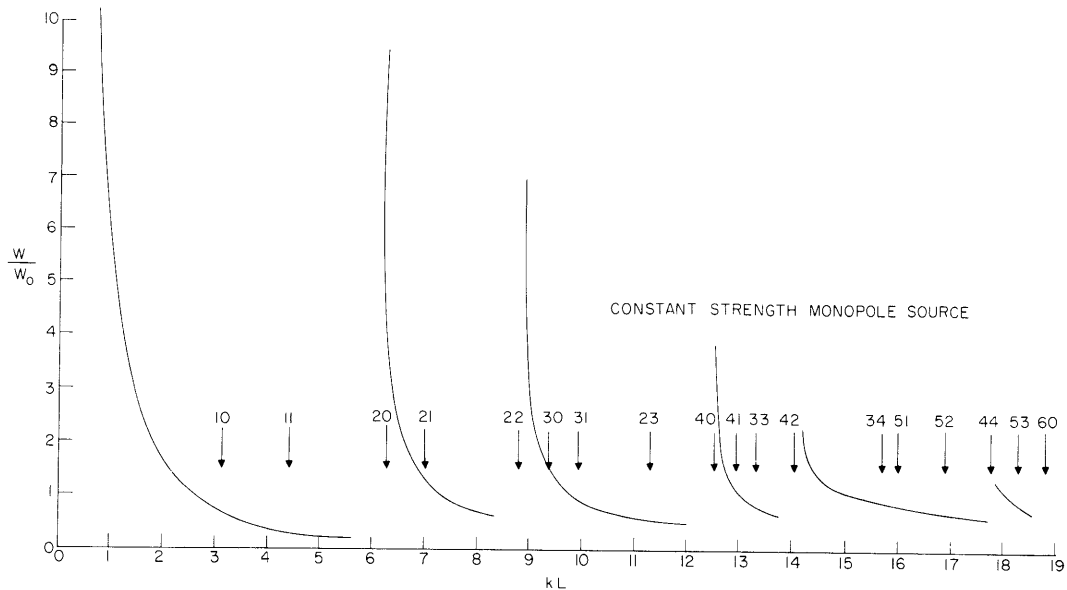


Fig. VIII-3. W/W_0 vs kL for a source in the center of a hard duct.

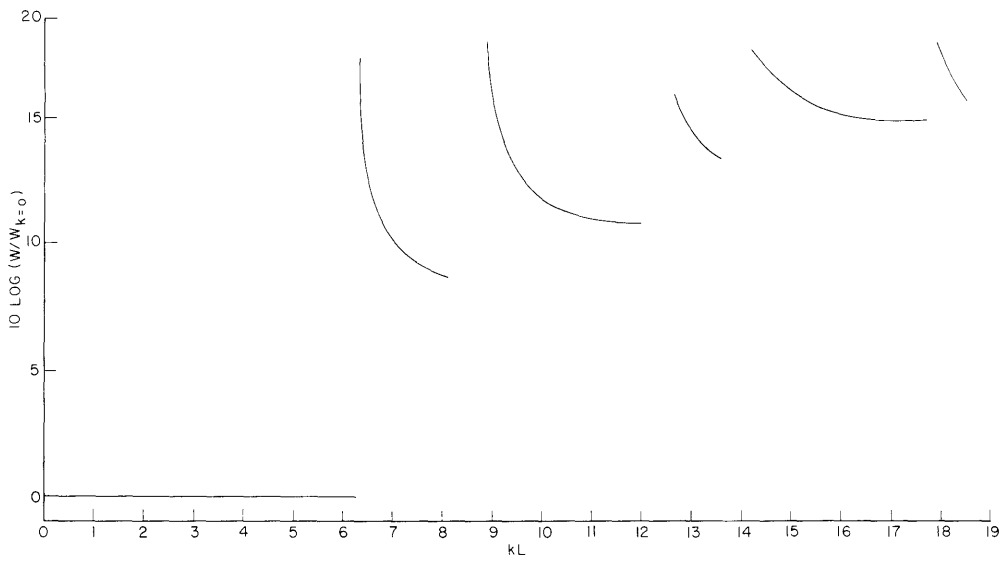


Fig. VIII-4. $W/W_{k=0}$ vs kL for a source in the center of a hard duct.

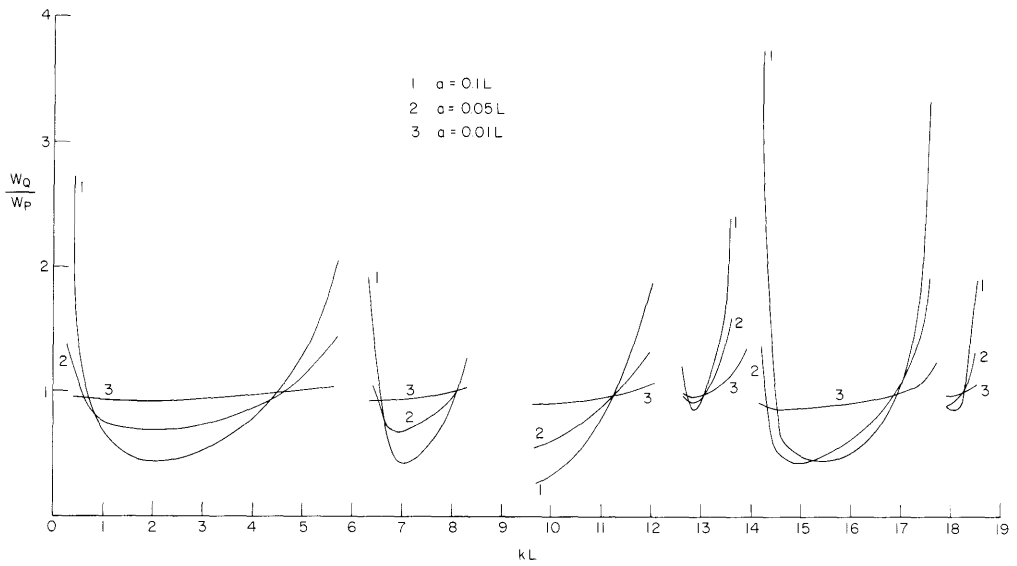


Fig. VIII-5. W_Q/W_P as a function of kL .

(VIII. PHYSICAL ACOUSTICS)

according to Eq. 3, the ratio W/W_0 is the same for either type of source if $a = 0$. For $a \neq 0$, the image method is only approximate, but should be valid, provided that the source size (a) is small compared with the x (or y) dimension (L) of the square duct.

The ratio W_Q/W_P has been plotted in Fig. VIII-5 for three values of a , $a = 0.01 L$, $a = 0.05 L$, and $a = 0.1 L$. Here, W_P is the output of a constant pressure source, and W_Q is the output of a constant strength (volume velocity) source.

It can be seen from Fig. VIII-5 that for small sources the power output of a constant-pressure source is nearly the same as for the constant-strength source. For larger sources, the difference between the two types becomes greater. Since the image description is strictly valid only for very small sources, no calculations were made for values of a/L greater than 0.1.

G. C. Maling, Jr., U. Ingard

References

1. U. Ingard and G. L. Lamb, Jr., J. Acoust. Soc. Am. 29, 743 (1957).
2. R. V. Waterhouse, J. Acoust. Soc. Am. 30, 4 (1958).
3. D. R. Grine, Quarterly Report, Acoustics Laboratory, M. I. T., July-September 1957, p. 15.
4. G. C. Maling, Jr., Quarterly Progress Report No. 51, Research Laboratory of Electronics, M. I. T., October 15, 1958, pp. 107-110.
5. G. C. Maling, Jr., J. Acoust. Soc. Am. 31, 115 (1959).
6. G. C. Maling, Jr., J. Acoust. Soc. Am. 36, 781 (1964).
7. R. V. Waterhouse, J. Acoust. Soc. Am. 35, 1144 (1963).

D. STUDIES OF SHOCK STRUCTURE

The observation of hydraulic jumps to shed light on the structure of collisionless shock waves in plasma was reported in the last quarterly report.¹ These previous experiments showed that neither the "thinnest shock hypothesis" nor the "thickest shock hypothesis" has general validity. The experiments have continued. The new results, when carried over to the plasma and coupled with some new plasma theory, contain some novel features.

Hydraulic-jump structure has been examined at various water depths as a function of Mach number. At small Mach numbers, below $M = 1.25$, the structure is characterized by waves whose length is fairly long, compared with the depth of water. These waves are a permanent feature of the jump structure, in that they travel at exactly the same speed as the jump, and so they stand still in jump coordinates. If gravity is the predominant restoring force, these waves stand behind the jump; if, on the other hand, surface tension is the predominant restoring force (this can be obtained experimentally

by reducing the water depth to approximately 0.5 cm), then they stand ahead.

These results can be carried over to plasma. There are plasma waves, the magnetoacoustic waves, which have all of the essential properties to make them a permanent feature of the collisionless shock wave, like the long surface waves in shallow water. Thus, the existence of finite-amplitude magnetoacoustic waves that stand in shock coordinates is expected.

Some simple theorizing about these waves and their role in the collisionless shock leads to the following predictions: If the magnetic field is perpendicular, or almost perpendicular, to the direction of the shock, the waves will stand behind the shock front, and will be of approximate length $\sqrt{m_e/m_i} r_i$, where m_e and m_i are the masses of electron and ion, respectively, and r_i is the gyroradius of an ion moving at the magnetoacoustic speed. If, on the other hand, the magnetic field lies away from the plane perpendicular to the shock direction, the waves will stand ahead of the shock front, and will be of approximate length r_i . The transition between these regimes is smooth, and occurs when the magnetic field is at an angle $\sqrt{m_e/m_i}$ away from the plane perpendicular to the shock direction.

As the strength of hydraulic jumps is increased, the long wave becomes of such large amplitude that it breaks, and the character of the hydraulic jump changes. Surface turbulence now appears, as does a different wave, of much shorter wavelength. This second wave, like the long wave that appears for weaker jumps, stands still in jump coordinates. The excess energy carried by the supersonic flow into the jump front is no longer converted to waves that carry the energy downstream; instead, the energy is dissipated right at the jump front by viscous damping of the surface turbulence and standing waves. There are two outstanding features in these stronger jumps. The fact that the long wave is no longer excited and its consequences in the case of plasma shocks was discussed in the previous report.¹

Another feature is the pronounced tendency for short-wavelength waves traveling at the same speed as the hydraulic jump to be excited, as well as the fact that the scale of turbulence is largest around this wavelength. The three ingredients necessary for this behavior are: (i) the long wave breaks, if strong enough; (ii) short-wavelength waves traveling at the jump speed are possible; and (iii) standing waves are preferentially excited.

These three ingredients are also present in the collisionless plasma. I can argue on quite general grounds that waves whose phase velocity is the same as the source speed (the shock front being the source, in this case) are preferentially excited, no matter what the medium. As the amplitude of long (that is, of order r_i or $\sqrt{m_e/m_i} r_i$) waves increases, because of increasing Mach number, such long waves become unstable, and so they "break" into smaller wavelength disturbances. The wavelengths that can stand are of order $(m_e/m_i)r_i$ and of order $(\omega_c/\omega_p)r_i$, where ω_p/ω_c is the ratio of plasma

(VIII. PHYSICAL ACOUSTICS)

frequency to ion-cyclotron frequency. The former mode is an electron-cyclotron wave; the latter is an electrostatic oscillation. Their presence is expected for strong collisionless shocks, and their decay by Landau damping and collisional damping should provide the energy dissipation associated with the collisionless shock wave.

J. M. Witting

References

1. J. M. Witting, Studies of shock structure, Quarterly Progress Report No. 73, Research Laboratory of Electronics, M.I.T., April 15, 1964, pp. 27-28.